XVI IMEKO World Congress
Measurement - Supports Science - Improves Technology - Protects Environment ... and Provides Employment - Now and in the Future
Vienna, AUSTRIA, 2000, September 25-28

GEOMETRY EFFECT OF INDENTERS ON DYNAMIC HARDNESS

V. Vasauskas
Department of mechanics of solids
Kaunas University of Technology, LT-3028 Kaunas, Lithuania

Abstract: The present paper reports on the underlying concept for securing the measuring basis used in the method of dynamic hardness. The dynamic hardness was evaluated from measurements of residual contact dimensions as a function of impact velocity and continuous force - displacement curves over the velocity range 5 to 40 m.s^{-1} for various geometry of indenters. The value for several engineering metals obtained dynamic hardness was 1,12-1,40 higher than the static hardness. The higher hardness in impact causes more extensive elastic recovery and smaller plastic zone surrounding the contact site.

Keywords: dynamic hardness, indentation angle, stress-strain curve

1 INTRODUCTION

In recent years there has been a renewed interest in dynamic indentation hardness technique [1-4] because of its simplicity, low cost and relevance to the behaviour of structures subjected to impact wear, high speed forming, high velocity sliding wear, crash, etc. Analogous to static indentation dynamic indentations can be used to predict plastic properties of materials at high strain rates, precisely controlled and directly measured, typically in the range of 10^3/s. To obtain quantitative information regarding the elastic, plastic and fracture behaviour of systems, a range of indenter geometry's may need to be used (e.g. hemispherical indenter for elastic behaviour, pyramids primarily for the plastic response, sharper indenter for fracture response, etc.). Regular sharp indenters are usually in the shape of pyramids of square base (Vickers), triagonal base (Berkovich) and rhomboid base (Knoop), or in conical shape (Rockwell). Non-regular blunt indenters are spherical indenters (Brinell). Thus, work - hardening characteristics of the material are manifest as a variation of hardness with indenter geometry and it is sometimes difficult or impossible to interpret.

In an dynamic indentation hardness test, geometry of the test is actually being controlled by the various properties of the material that are of interest, e.g., the hardness, Young's modulus, or strain - rate sensitivity. The effective stress is taken to be the contest pressure or hardness, and the shape of the indenter and the displacement rate determine the effective strain rate [5,6]. Although the magnitude of the indentation pressure is correctly predicted, it is often stated that the mode of deformation, which is observed with a blunt indenter, is very different from the theoretical pattern. The development of continuous indentation systems, offer the opportunity to obtain a dynamic indentation parameters at each stage of impact process [3,7]. There are two important innovations in this system: (1) the indentation is described in terms of continuous measurements of applied load and penetration depth, and (2) the indentation can be performed over a wide range of loading times from hours to milliseconds. The objective of the present paper is to describe a novel technique for characterising the dynamic hardness of materials, which employs one of the standard indentation methods, and various indenters geometry.

2 BASIC THEORETICAL ASPECTS

There is a fundamental difference between static and dynamic hardness testing: in static tests the effective force acting on the penetration indenter is clearly and comprehensively determined throughout the entire process of penetration into the specimen. The corresponding predetermined data with the dynamic hardness method are the impact velocity, the mass and overall elasticity of the impact indenter. However, these three parameters define the applied force, i.e. the penetrating stressing, clearly and comprehensively only at the start of penetration (start of impact). In this case still remain a number of unresolved questions about the geometry of the indenters, the direction of flow of the displaced material, the meaning of the "representative strain" and others [5,6]. Both the rigid-plastic theory and the expanding cavity theory of indentation require that the distribution of contact pressure across the face of the indenter should be uniform. Data indicate that this requirement is met only when the indenter angle is acute $(2q > 120°)$ and when the ratio E/Y is high. For obtuse indenters,

such as those with which we are concerned, the pressure distribution exhibits a high central maximum. The effective included angle $2q$ of an indenter plays a very important role in this case. The effective indenter angle generally does not remain constant with the axial length. This error increases rapidly with the indenter angle due to a tan0 term, which defines the imposed strain. With indenters of regular geometry the mean contact pressure is load independent ("geometrical similarity") and accordingly gives a measure of the materials hardness ($H = F / a_0 a^2 =$ constant, where F is the load, a characteristic dimension of the impression, and a_0 an indenter geometry constant). The indentation does not change shape as the indenter progresses into the specimen and the mean pressure to produce plastic flow is almost independent of the size of the indentation. It has been suggested by Tabor [2], that all impressions can be compared under geometrically similar conditions, namely, at d/D ratio of 0,375 for the spherical indenter. At this particular value of d/D, the include angle of the tangents to the sphere at the edge of penetration is equal to the angle between opposite faces of the pyramidal Vickers indenter namely 136°.

Chiang et al. [5] here shown that the global stress field around an indenter is determined by the indentation volume d V. Since the shape of the indented volume is not much important for the stress field outside the plastic zone, the models suppose the indented volume (d V) to be hemispherical (see Figure 1). Thus the indentation volume

$$dV = (2p/3)h^3_{\max} = 2p/3[mV^2_{ind}(n+1)/2a]^{3/n+1} \quad (1)$$

where a and n are constants, which must be obtained experimentally.
Equating normal component of the striker kinetic energy (R with the work done during impact we obtain

$$W^n_{kin} = m_s V^2_{ind}/2 = \int_0^{h_{\max}} F(h)dh = H \int_0^{h_{\max}} A_{ind}(h)dh = HdV \quad (2)$$

Our deformation model, assume that the volume of impression produced by the impact indenter, is proportional to the kinetic energy, W, of the indenter but is independent of its shape or tip angle, $2q$. Since the volume of a right cone with an apex angle of $2q$ is

$$V = \frac{p}{24}\cot q\, d^3 \quad (3)$$

where d is the diameter of the bottom of the right cone

$$W = V.W_0 = \frac{p\,W_0}{24}\cot q\, d^3 = W_0 k d^3 \quad (4)$$

where W, is the assumedly constant kinetic energy absorbed per unit volume of deformed metal, and $k = p\cot q/24$, a geometric constant.

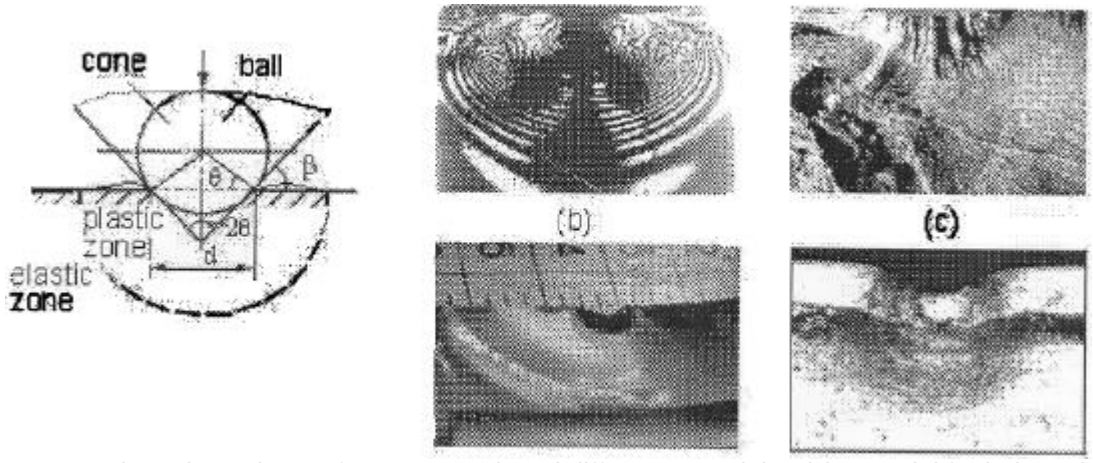

Figure 1. Indentation volumes for cross-sectioned different materials: (a) - model for indentation, (b) - elastic field. (c) - thermoplastic, (d) - PMMA, (e) - TiN coating (x80)

This assumption is consistent with the idea that the residual driving force for indenter is derived from an elastic accommodation of the hardness-impression volume and that the influences of indenter geometry and the indentation load on the residual driving force are completely characterised by the hardness-impression volume. An empirical relation has expressed the relation between the hemispherical plastic zone size relative to the hardness-impression volume and the elastic (E,n) and

plastic (hardness, H) properties of the indented material

$$b = \left[\frac{E}{H}\right]^{1/2} \frac{d}{2\left(\sqrt{2}p\,\tan q\right)^{1/3}} \tag{5}$$

where b is the radius of the hemispherical plastic zone, d the diameter of the hardness impression, and $2q$ the apex angle of the indentation cone angle.

The complete dynamic indentation procedure may be presented into the three following stages: starting phase, indentation phase and rebound phase. During the striking phase the potential energy of the test specimen is converted into kinetic energy either by free fall or by a spring (Figure 2). Thus for a given contact geometry the intrinsic coefficient of restitution is uniquely determined by the degree of recovery and useful measure of the degree of reversibility of contact deformation. An equivalent expression for the apparent hardness under conditions of impact loading is given by $H_d = W_0/V_0$, , where H_d is the dynamic hardness, W, - initial kinetic energy absorbed in plastic deformation and V, is the volume of permanent indentation. Energy loss or respectively the residual energy is dependent on the plastic and elastic characteristics of the specimen.

If we accept that the strain produced by a cone is equal to that produced by a ball or square - based pyramid of the same apex (indentation) angle, then the strain produced by a Vickers pyramid indenter is given by $e = 0{,}2\cot\frac{1}{2}(136°) \approx 0{,}08$. This agrees very well with the empirical finding by Tabor [2] that a Vickers pyramid induces a strain of between 8 and 10 percent. We have derived [7] the following equation to describe the plastic deformation of a recovered indentation volume in terms of the indentation diameter (depth):

$$e = \frac{A_1 - A_0}{A_0} = \left(\frac{p\,d^2}{4\sin q} - \frac{p\,d^2}{4}\right) / \frac{p\,d^2}{4} = \frac{1}{\sin q} - 1 = \ln\frac{1}{\sin q} \tag{6}$$

where e - average contact deformation, $A_1 = p\,d^2/4\sin q$ - surface of indentation, $A_0 = p\,d^2/4$ - projection area indentation, $2q$ - indentation contact angle, d - diameter of indentation.

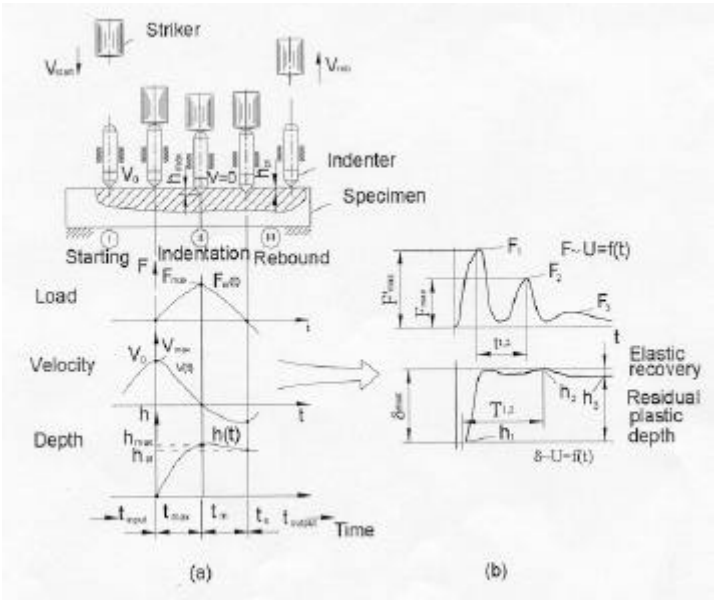

Figure 2. Dynamic indentation phases for triple "striker - indenter - specimen" system

There are two main categories of dynamic hardness methods namely "rebound" methods and “reaction-force" methods [2-4]. In the case of the former type, hardness is measured on the basis of the energy absorbed by the test-piece during impact and, in the case of the latter type, on the basis of the reaction force exerted on the indenter by the test piece. There are, in turn, two types of rebound test. The first is the well-known scleroscope test in which the energy loss is measured by the height of rebound of the impact indenter. The second is the energy quotient return (FQUO) method where the energy loss is calculated electronically from the ratio of the velocities of the indenter before and after impact.

Three general categories of impact analysis may be distinguished: a) stereo mechanical analysis; b) Herz (quasi - static) analysis, and c) analysis including vibration effects. Quasi-static conditions will

be obtained if, at first, the impact duration must be long enough for of one wave across the contact area, i.e. when $t_c \ll t_{imp}$ (t_c - indentation contact time, t_{imp} - impact duration), quasi-static conditions are met with regard to the indenter. The second condition is that quasi-static state should be realised in the specimen material too. This condition will be met if the impact duration (t_{impx}) is considerably greater than the time required for the elastic waves in the specimen to travel some characteristic length associated with the deforming volume (t_s). For different specimen materials and in the case of $v \leq 100$ m/s impact duration is 15-20 times longer than t_s quasi-static assumptions are realised in the specimen.

3 EXPERIMENTAL

Figure 3 is a schematic of the experimental set-up designed in deliver a single, controlled dynamic indentation into a specimen material. The measurement system consists of an impact device and an electronic indicator device [7]. The impact device fires the striker against the material to be tested in system striker - indenter - specimen. A piezoelectric transducer sensed loads, while the displacement was determined from the indenter travel recorded by means of the photocell. After further amplification, the signals are analysed for member of counts and intensity (ADS - 10 bits). Functions F(t) and d (t) are accounted for 256-1024 dots. Interval between dots 10-40 μs. Data acquisition and evaluation are performed by means of a minicomputer allowing also graphic display and hard copy output. Choosing striker bars of various lengths can vary the duration of the input pulse. Changing the stiffness of the spring and thus changing the impact velocity of the striker bar can vary the amplitude of the incident compression stress pulse (or the incident load).

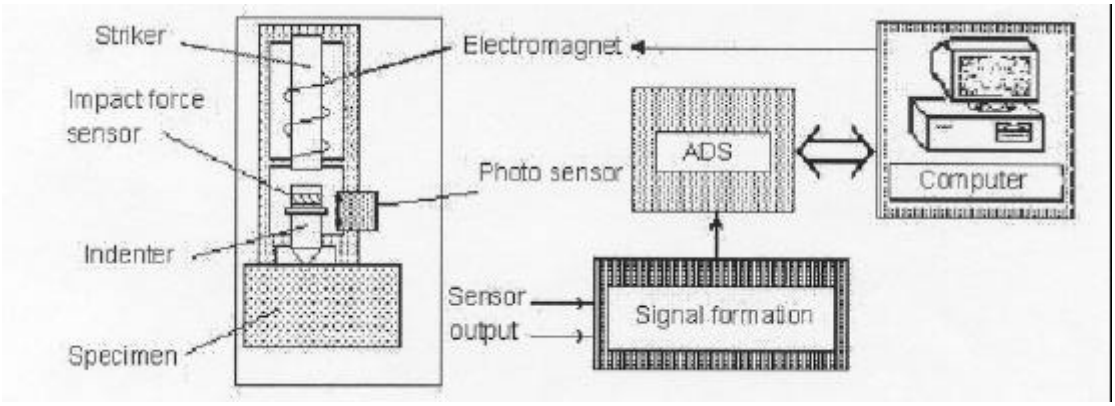

Figure 3. Schematic of the experimental set-up for dynamic indentation

An examination of the energy balance during the impact indicates that at least 70-80% of the initial kinetic energy of the indenter is dissipated only in plastic deformation in the specimen. The kinetic energy of the rebounding is estimated from measured coefficients of restitution depending on indentation geometry, impact velocity and specimen material. Thus, $W_0 = W_1 \cdot h_0$, where W_1 - all accumulated initial kinetic energy of striker, h_0 - total efficiency for the striker-indenter-specimen set is $h_q = h_1 \cdot h_2$ where h_2 - loss of energy at the indenter-specimen impact for non-linear plastic deformation of cone indenter. According to Figure 2 we have

$$h_2 = (1 - C_q^2)\frac{m_1}{m_1 + m_2} \tag{7}$$

where C_q - restitution factor as function of indenter angle $2q$, m_1, - striker mass, m_2 - indenter mass.

For m_1/m_2=0,5 and cone angles $2q = 90° \div 160°$, $h_1 = 0{,}5 \div 0{,}46$. Then total efficiency of the dynamic system in our experiments was for various indentation angles in the ranges $0{,}336 \div 0{,}500$.

4 RESULTS AND DISCUSSION

Results show that when an indentation is formed in a specimen by an impact, the pressure resisting indentation is greater than that occurring in the formation of a similar indentation under static conditions. It is apparent from these equations and from the experimental curves that in general the coefficient of restitution of impacting solids capable of undergoing plastic deformation will not be a constant. As the indentation angle decrease, and there will be a corresponding decrease in the coefficient of restitution. Increasing the indenter tip angle should lead to an increase in the work done in penetration. The increase in work is small but significant at low cone angles.

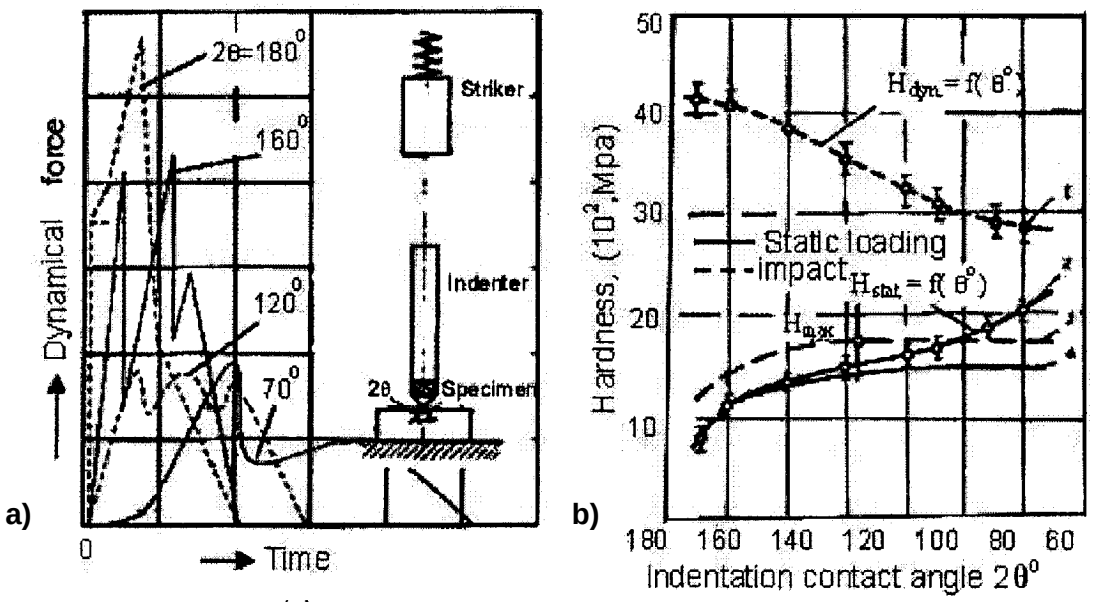

Figure 4. Triple dynamic hardness measurement system and force - time curves for various indentation angles (a) and stress-strain curves for static and dynamic indentation hardness (b): 1,2-contact friction unaccounted, 3,4-contact friction and efficiency of dynamic system striker-indenter-specimen set accounted

At large cone angles this simplified approach must break down. Probably the most significant factors causing this disagreement are work hardening of the material and variation of the flow conditions with indenter geometry. Thus, increasing the indenter ages angle should lead to an increase in the work done in indentation. The increase in work is small but significant at low indentation angles. At large indentation angles this simplified approach must break down.

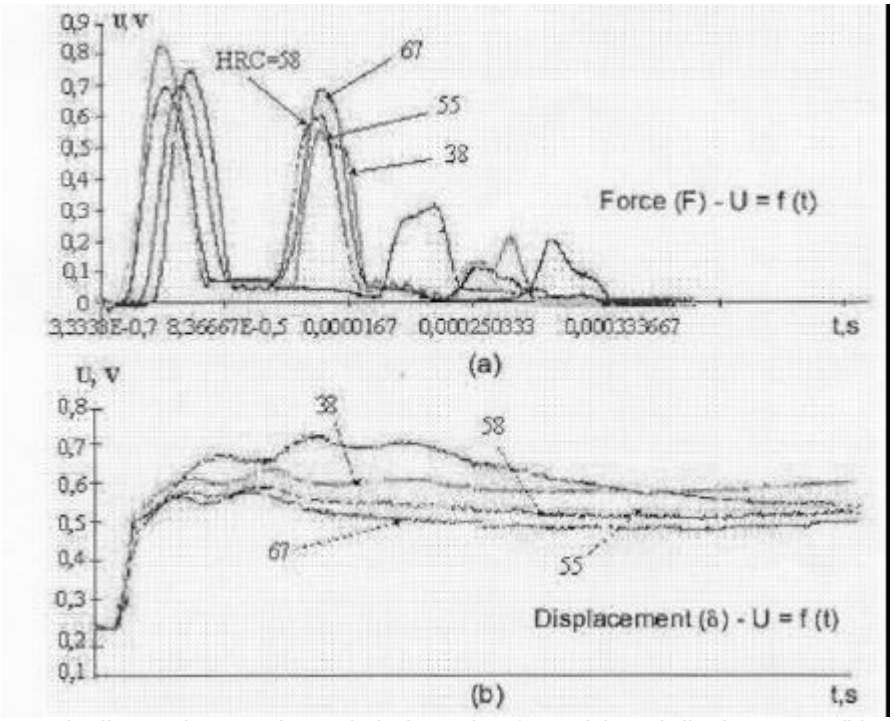

Figure 5. Typically continuous dynamic indentation force (a) and displacement (b) curves for cone $2q$ =90° and steel of various hardness (HRC=23 – 63)

Also we see that value of the friction affects the magnitude of the mean pressures necessary to form the indentations and position of the maximum. Friction exerts the biggest influence at small angles and is far less important in the "compressive" mode of the large angled indenters.

The static hardness is observed to increase as the deformation size increases, indicating that a certain amount of strain hardening has occurred. In dynamic conclusion we have, at first, that when deformation size increases hardness (Figure 4b, curve 1) decreases. Dynamic hardness is 1,12-1,40 times higher the static hardness, because of the effect of strain rate on the deformation of Material. Superimposing the spherical results onto the cone penetration curve suggests that indenters with included angles 120° generate plastic strain levels within the invariant range. Hence, the penetration pressures attained with indenters of the regular shape should correlate with the pressures that pertain for hemispherical indentations. This is the basic requirement for relating experimental indentation results to the reference geometry.

The dynamic hardness-strain curve can be converted to the conventional tensile or compressive flow stress (s) vs plastic strain curve by simply dividing H_d by the constraint factor c [2,7]. Constraint factor is defined as the ratio of hardness to s at a constant strain and has been shown to be a valid concept under static indentation conditions. The curves have a typical extremum shape in the region of indentation angles from 100° to 120°, which corresponds to point H_{max}. From our data this degree of deformation corresponds to the calculated ultimate strength. The method is based on the idea that 90°-cone impressions are more closely related to the static stress-strain or flow curve at the maximum load than are the commonly used indentations according to Brinell, Vickers or Rockwell. The fact that the indentation data lie close to straight lines in the region $2q$ <120°) is consistent with the assumption that constraint factor is practically a constant over the whole range of strains. In the light of these results it is clear that while the analysis just given might be capable of explaining the dependence of the measured hardness of indenter angle for annealed or lightly worked materials, it cannot explain observations made when heavily worked materials are indented.

5 CONCLUSIONS

The dynamic hardness was evaluated from measurements of residual impact impressions, continuous force-displacement curves and the impact velocity. This was achieved by use of a controlled contact geometry, which displayed geometrical similarity with penetration. The dynamic hardness was found 1,12-1,40 higher than hardness determined by static indentation. The present model provides a useful way to calculate the coefficient of restitution and the critical deformation in both elastic and plastic regimes, based on the energy loss models and the energy conservation principle for various geometry of indenter.

Although the morphology of the damage surrounding the contact site is similar in static loading and impact, some differences in the extent of damage were identified. A larger extent of elastic recovery in the depth of the residual contact impression and a smaller plastic zone size relative to the contact dimension are both associated with the higher ratio of hardness-to-modulus in impact and “representative strain" which is controlled by indentation angle. The mechanism of impact-energy transformation seems to be more complicated than that of metal deformation.

REFERENCES

[1] Y. Tirupataiah and G. Sundarajan, A dynamic indentation technique for the characterisation of the high strain rate plastic flow behaviour of ductile metals and alloys, *J. Mech. Phys. Solids* 39 (2) (1991) 243-271
[2] D. Tabor, A simple theory of static and dynamic hardness, *Proc. R.Soc. London* 192A (1948) 247-274
[3] D. Leeb, Definition of the hardness value "L" in the EQUOTIP dynamic measuring method, in: *Hardness testing in theory and practice,* (VDI-Berichte, 583)-Düsseldorf, 1986, p.109-135
[4] P.F. Aplin, Classification and selection of portable hardness-testing equipment, in: J. Boogaard and S.M. Van Dijk (ed.), *Proceedings of the 12th World Conference "Non-Destructive testing".* (Amsterdam, 1989), The Netherlands, 1989, p. 683-688
[5] S.S. Chiang et al., The Response of Solids to Elastic/Plastic Indentation. I. Stresses and Residual Stresses *J. Appl. Phys.* 53 (1) (1982) 298-311
[6] K.L. Johnson, A correlation of indentation experiments, *J. Mech. Phys. Solids* 18 (1970) 115-126
[7] V. Vasauskas et al., Contact mechanical state control in manufacture, in: M.B. Zaremba (ed.), *Proceedings of the 7th IFAC/IFIP/IFORS/IMACS/ISPE Symposium "Information Control Problems in Manufacturing Technology"* (Toronto, Ontario, 25-28. May 1992), Canada, v.II, 1992, p.567-572.

AUTHOR: Ass. Prof. Dr. Vytautas VASAUSKAS, Department of mechanics of solids, TU Kaunas, Mateikos str. 1-4, LT-3028, Kaunas, Lithuania, Phone 370-7-22-46-03, Fax 370-7-22-16-08
E-mail: rastine@cr.ktu.It